AUTHOR(S):

TITLE:

YEAR:

Publisher citation:

OpenAIR citation:

Publisher copyright statement:

This is the _____ version of proceedings originally published by _____
and presented at _____
(ISBN _____; eISBN _____; ISSN _____).

Modelling Multiphase Flow in Vertical Pipe Using CFD Method

David Alaita[1*], Mamdud Hossain[1], Sheikh Zahidul Islam[1]

[1]School of Engineering, Robert Gordon University, AB10 7GJ, Aberdeen, UK.
[*]d.a.alaita@rgu.ac.uk, m.hossain@rgu.ac.uk, s.z.islam1@rgu.ac.uk

Abstract

Investigations of gas-liquid-solid flows in large diameter vertical pipes are scarce and detailed three phase flow study is still required to understand the flow interactions. Further investigation using high fidelity modelling is thus necessary due to complex flow interactions of the phases.

In this study, a Computational Fluid Dynamics (CFD) method is used to investigate multiphase gas-liquid-solid flow in vertical pipe. Firstly, an appropriate validated numerical simulation scheme for two phase gas-liquid flow using ANSYS Fluent has been used to simulate possible flow regime transitions in vertical pipe. The scheme could predict the various flow regimes spanning bubbly to annular flow without prior knowledge of the flow patterns.

The scheme was further extended to investigate the impact of solid particles in the flow field. More importantly the impact of solid concentration on the flow regime development and sand deposition was investigated. The results showed that the particulate deposition is greatly influenced by the particle concentration. In addition, the regime transitions and development in gas-liquid flows are different than that of gas-liquid-solid flows.

Keywords: Vertical pipe simulation, Sand transport, Interfacial area concentration, Mass flux, Large diameter pipe, Solids deposition, gas-liquid-solids, Fluidization, CFD, Multi-fluid VOF.

1   Introduction

Multiphase flow is common in the petroleum industry as well as geothermal, nuclear energy and petrochemical industries. Production of oil and gas has become increasingly complex due to this type of flows resulting from sandstone reservoirs, ageing and deeper offshore exploration and production. This has led to many multiphase flow challenges to the oil and gas companies. In the past five decades, researchers have carried out various experimental studies to understand multiphase flow phenomenon. The complexity of resolving the interface forces and momentum transfer terms have lead researchers to develop mechanistic models to predict multiphase flow hydrodynamics

parameters. However, this approach has not yielded exhaustive results due to wide range of flow conditions and the complex interactions of the phases.

Researchers such as [1, 2], and many others have published comprehensive flow pattern prediction models that can be used to generate simple regimes but, these models have not included the present of solid particles. Hence accurate prediction of multi-components flow hydrodynamics is still required. According to [3], reliable predictions would involve accurate understanding of the physical mass transfer between the phases and physical properties of each phase.

Due to the increase demand in nuclear and oil and gas industries, the requirement to migrate toward larger diameter sizes for development has become essential [4]. While the applications of tools and correlation for large diameter pipes are different than small diameter pipes, most research carried in larger diameter pipes did not include the present of solids particles. Whereas a typical multiphase flow would contain gas-liquid-solid flows and detailed multi-dimensional models are needed to understand the complex flow dynamics [5].

Recently, researchers such as, [6-14], and others have studied two phase gas-liquid flows and had developed appropriate flow maps for large diameter pipes. However, the presence of solids particles and its impact on the pressure gradient, liquid & gas holdup and regime transition were not taken into consideration.

Investigation of the hydrodynamics of three phase gas-liquid-solid particles in vertical pipe, both experimental and computational fluid dynamics methods are rare in literature. Researchers have not paid much attention to the hydrodynamics of the multi-dimensional phasic flows in vertical pipes. For efficient transportation of sand particles from the wellbore to the surface via vertical and incline pipes, effective fluidization must take place. Ineffective fluidization may lead to sand deposit at the bottom of the pipe.

Hence in this investigation, an alternative modelling scheme in CFD has been used to simulate regime transitions in vertical pipe. The Eulerian Multi-fluid VOF with interfacial area concentration has been used in the initial case study and validated against experimental result. The scheme was then extended to investigate the impact of sand particles in the flow field and regime transitions. The concept of mass flux has been investigated and notable changes that occur in the particulate deposition has been analyzed. Phase transition is critical in oil and gas flows in vertical pipes [15], as shown in Fig.1, hence a CFD model capable of predicting different time-phased regime is required to understand the hydrodynamics of multiphase flow of oil and gas fluid [16]. The novelty of the report is that mass flux is a key determinant of particle deposition in oil and gas production. Establishing the threshold will be useful in the diagnosis of deposition and wellbore fill.

This paper is arranged into six sections. Following this introduction, the simulated cases are described in the second part. The third part contains the numerical methodology followed by the associated mathematical model in the fourth section. Lastly, the results and discussion are presented in the fifth section and conclusions in the sixth section of this paper
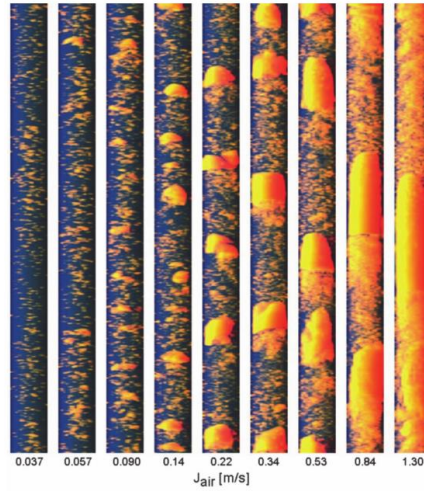
Fig. 1. Typical oil and gas flow regime transition (Adapted from Lakehal, 2013).

2 Simulation Case.

The simulation case was the experimental work of [9]. The experimental set up consist of a 52m vertical pipe of 189mm in diameter. The test fluid were Nitrogen gas and Naphtha, details are shown in Table 1. Four experimental cases were conducted and the flow regimes identified are shown in Table 2. However, due to the limitation of the CFD modelling, only 30 diameters of the length were used in the CFD model. This is the length at which fully developed flow is expected to be achieved.

Table 1. Fluid properties

Fluid Properties						
Pres-sure	Tempt	Density		Viscosity		Surface Tension
(bar)	(deg C)	Gas (kg/m^3)	Liq-uid(kg/m^3)	Gas (pa. s)	Liquid (pa. s)	N/M
20	30	23.4	702.3	1.77e-05	3.59e-04	0.0185

Table 2. Flow conditions and Regimes identified

Flow conditions and flow regimes identified		
Cases	Gas Superficial Velocity (m/s)	Flow Regimes Identified
Case 1	0.1	Bubbly
Case 2	0.21	Intermittent (Churn Turbulent)
Case 3	1	Semi -annular
Case 4	4	Annular
Liquid Superficial Velocity = 0.05m/s		

2.1 Geometry and Mesh

The initial step of the solution procedure is the generation of the geometry and mesh. The computational domain is a large vertical pipe of height 5.67m and a diameter of 0.189m. The geometry was created with Design Modeler and later exported to ICEM CFD 17.0 meshing software. The mesh was generated using the O-grid method, then the inlet was split for gas and liquid inlet boundary conditions. Fig. 2 shows the geometry and inlet gas and liquid entrance.

3 Methodology

A computational dynamics approach using ANSYS Fluent software is utilized to investigate the effect of sand particles in multiphase gas-liquid-solid flow. The method uses the Eulerian Multi-fluid VOF to investigate the transient hydrodynamics effect of multiphase flow.

To simulate the transient effect and flow regime evolution, the interfacial area transport equation (IATE) was utilized to model the change in interfacial area concentration (IAC) by accounting for the interaction of bubbles at reasonable boundary conditions. This eliminate the need for prior knowledge of the flow patterns. The validated CFD- model was extended to investigate the 3-phase gas-liquid-solid flows.
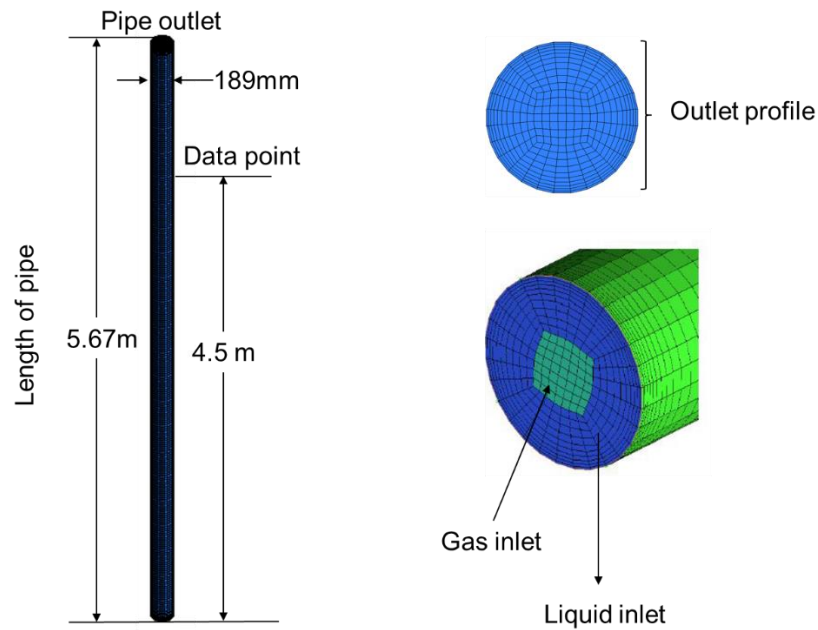
Fig. 2. Geometry and mesh

4 Mathematical Model

The mathematical description used to predict the multiphase flow is based on the energy balance equation for three phases. The Eulerian multi-fluid VOF considers the three phases to be interpenetrating continuum.

4.1 Mass Balance Equation

Gas:

$$\frac{\partial \rho_g \alpha_g}{\partial t} + \nabla \cdot \left(\alpha_g \rho_g \vec{v}_g \right) = 0 \tag{1}$$

Liquid:

$$\frac{\partial \rho_l \alpha_l}{\partial t} + \nabla \cdot \left(\alpha_l \rho_l \vec{v}_l \right) = 0 \tag{2}$$

Solid

$$\frac{\partial \rho_s \alpha_s}{\partial t} + \nabla \cdot \left(\alpha_s \rho_s \vec{v}_s \right) = 0 \tag{3}$$

Where:

$$\alpha_g + \alpha_l + \alpha_s = 1 \tag{4}$$

4.2 Momentum Balance Equation:

Gas:

$$\frac{\partial \left(\alpha_g \rho_g \overrightarrow{V_g} \right)}{\partial t} + \nabla \cdot \left(\alpha_g \rho_g \overrightarrow{V_g V_g} \right) = -\alpha_g \nabla p - \nabla \cdot \alpha_g \tau_g + \alpha_g \rho_g \vec{g} + M_{i,g} \tag{5}$$

Liquid:

$$\frac{\partial \left(\alpha_l \rho_l \overrightarrow{V_l} \right)}{\partial t} + \nabla \cdot \left(\alpha_l \rho_l \overrightarrow{V_l V_l} \right) = -\alpha_l \nabla p - \nabla \cdot \alpha_l \tau_l + \alpha_l \rho_l \vec{g} + M_{i,l} \tag{6}$$

The term on the right-hand side of Eqs. 5 and 6 represent pressure gradient, stress, gravity and interface force respectively.

Solid:

$$\frac{\partial \left(\alpha_s \rho_s \overrightarrow{V_s} \right)}{\partial t} + \nabla \cdot \left(\alpha_s \rho_s \overrightarrow{V_s V_s} \right) = -\alpha_s \nabla p - \nabla \cdot \alpha_s \tau_s - \nabla p_s + \alpha_s \rho_s \vec{g} + M_{i,s} \tag{7}$$

The solid momentum equation contains the solid pressure developed by [17, 18]. The stress tensor τ, for each of the three phases can be expressed as:

$$\tau_g = -\mu_{eff,g} \left[\nabla \overrightarrow{v_g} + \left(\nabla \overrightarrow{v_g} \right)^T - \frac{2}{3} \left(\nabla \overrightarrow{v_g} \right) I \right] \tag{8}$$

$$\tau_l = -\mu_{eff,l} \left[\nabla \vec{v_l} + (\nabla \vec{v_l})^T - \frac{2}{3}(\nabla \vec{v_l})I \right] \tag{9}$$

$$\tau_s = -\mu_{eff,s}[\nabla \vec{v_s} + (\nabla \vec{v_s})^T] + \left(\lambda_s - \frac{2}{3}\mu_{eff,s} \right) \nabla \vec{v_s} I \tag{10}$$

4.3 Closure Laws for stress and pressure:

The closure laws for the Eulerian model was derived from the Kinetic Theory of Granular flow as:

$$P_s = \alpha_s \rho_s \Theta_s + 2\rho_s(1 + e_{ss}) \alpha_s^2 g_{0,ss}\Theta_s \tag{11}$$

Where:

$$\Theta_s = \frac{1}{3}u_{s,i}^2 \tag{12}$$

$$g_{0ss} = \frac{s+d_p}{s} \tag{13}$$

$$\lambda_s = \frac{4}{3}\alpha_s^2 \rho_s d_s g_{0,ss}(1 - e_{ss}) \left(\frac{\Theta_s}{\pi} \right)^{\frac{1}{2}} \tag{14}$$

Where:
Θ = granular temperature, e = restitution coefficient, λ_s = bulk viscosity, $\vec{u_s}$ = particle fluctuating velocity, g_o = radial distribution function, s = distance between the grains, for dilute flows, $s \rightarrow \infty$, therefore $g_o \rightarrow 1$ and vice versa.

4.4 Closure laws for interface exchange momentum.

The resolution of the applicable interface exchange forces is very critical to successful modelling of multiphase flows. Various forms of empirical correlations for interface forces and assumptions are considered. Selection criteria is based on whether it is a fluid-fluid, fluid-solid and solid-solid exchange coefficient that is required. All exchange coefficients are functions of the drag function. To choose appropriate drag function depends on the drag coefficient. Because most interface coefficient are formulated for two phase flows makes it more difficult to understand the interface exchange in three phase multiphase flows.

From the Eqs. 5 -7, the M_i is the interface exchange momentum terms. The component of the interfacial forces includes the drag and the non-drag forces (Eq. 15). The drag is the dominant force that is accounted in this model.

$$M_i = F_d + F_{lift} + F_{wl} + F_{vm} + F_{td} + F_{ti} \tag{15}$$

Because the other forces are comparatively small, only the drag force is accounted for in this model.

4.5 Interfacial Transport Equation:

The inter-facial area concentration is defined as the inter-facial area between two phases per unit volume. It is a simpler form of population balance modelling which uses a single transport equation per secondary phase [12]. The transport equation for the interfacial area concentration (IAC) is given as (fluent theory guide)

$$\frac{\partial(\rho_g X_g)}{\partial_t} + \nabla.\left(\rho_g \overrightarrow{u_g}\, X_p\right) = \frac{\frac{1}{3}(D\rho_g)}{D_t}X_p + \frac{2}{3}\frac{m_g}{\alpha_g}X_p + \rho_g\,(S_{RC} + S_{WE} + S_{TI}) \tag{16}$$

Where X_p is the interfacial area concentration ($\frac{m^2}{m^3}$) and α_g is the gas volume fraction. The first two terms on the right-hand side of Eq. (16) are the gas bubble expansion due to compressibility and mass transfer (phase change). m_g is the mass transfer rate into the gas phase per unit mixture volume ($\frac{kgs^{-1}}{m^3}$). S_{RC} and S_{WE} are the coalescence and sink terms due to random collision and wake entrainment, respectively. S_{TI} is the breakage source term due to turbulent impact.

5 Results and Discussion

The initial step of the solution procedure is the generation of the geometry and mesh. The computational domain is a large vertical pipe of height 5.67m and a diameter of 0.189m. Four different gas velocities were investigated as indicated in table 2. The comparisons of the results were done using standard void fraction and Probability density function approach similar to [19].

5.1 Flow Structure Visualization

The contour plot in Fig. 3 (case 1-4) shows the flow development of the flow regimes at different superficial velocities: One simulation scheme was able to model bubbly flow (case 1), churn turbulent flow (case 2), semi-annular flow (case 3) and annular flow (case 4) regimes.
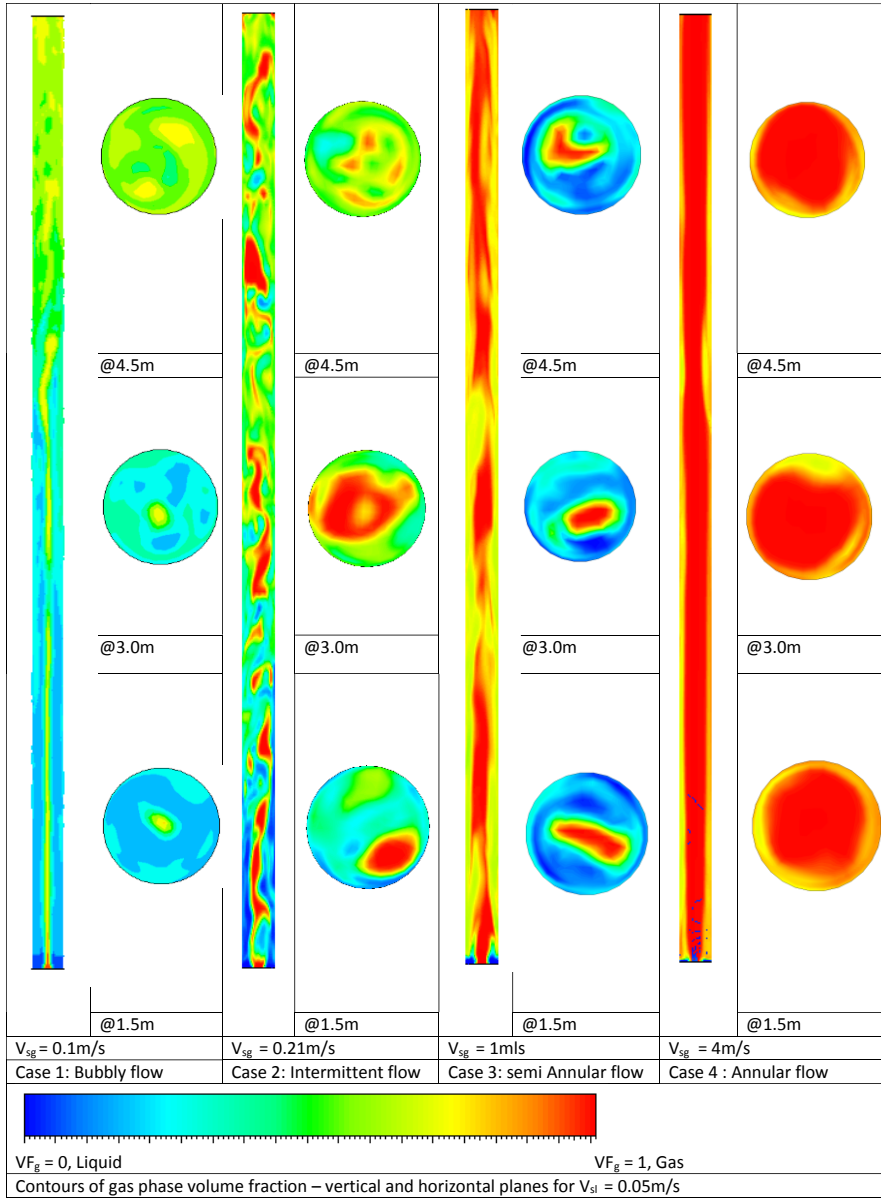
Fig. 3 . (Case 1 -4) Contour plot of the flow field

5.2   Time series Void Fraction Analysis

5.2.1   Superficial gas velocity of 0.1m/s.

Figure. 4 shows the void fraction plot for the experimental and CFD simulation results for the superficial velocity gas velocity of 0.1m/s and liquid superficial velocity of 0.05m/s. The void fractions for both the experiment and CFD cases are an average of 0.6 which corresponds to bubbly flow.
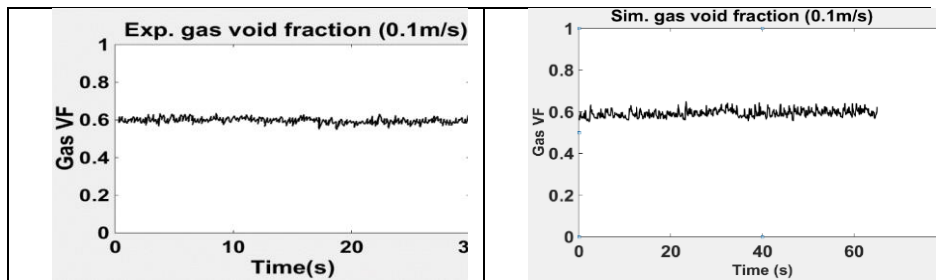
Fig. 4. Experimental and Simulation results: Liquid and gas superficial velocity: 0.05m/s & 0.1m/s.

5.2.2   Superficial gas velocity of 0.21m/s.

Figure 5 shows the void fraction plot for the experimental and CFD simulation results for the superficial gas velocity of 0.21m/s and liquid superficial velocity of 0.05m/s. The result shows intermittent (churn turbulent) flows as reported in the experimental results.   Area average void fractions of 0.64 -0.7 extracted from the simulation compared appropriately with experimental result.
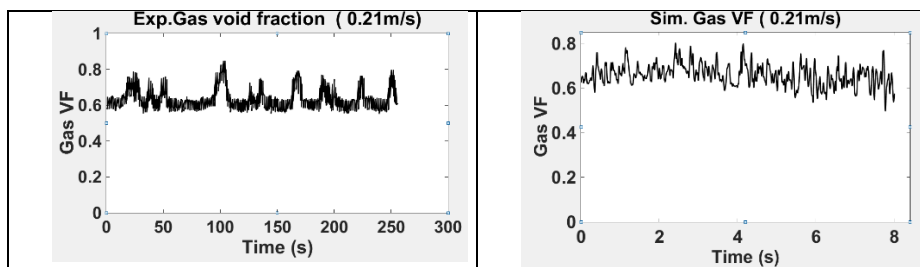
Fig. 5. Experimental and Simulation results: Liquid and gas superficial velocity: 0.05m/s & 0.21m/s.

5.2.3 Superficial gas velocity of 1m/s.

Figure 6 shows the void fraction plot for the experimental and CFD simulation results for the superficial gas velocity of 1m/s and liquid superficial velocity of 0.05m/s. The void fraction value of 0.77 - 0.85 indicates intermittent flows as reported in the experimental results. Area average void fractions extracted from the simulation thus compared appropriately with experimental results.
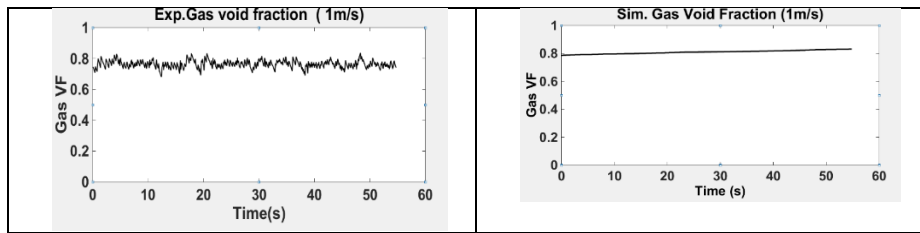
Fig. 6. Experimental and Simulation results: Liquid and gas superficial velocity: 0.05m/s & 1m/s.

5.2.4 Superficial gas velocity of 4m/s.

Figure 7 shows the void fraction plot for the experimental and CFD simulation results for the superficial gas velocity of 4m/s and liquid superficial velocity of 0.05m/s. Void fraction result is 0.95- 0.99 which indicates the signature of annular flows as reported in the experimental results. Area average void fractions extracted from the simulation thus compared appropriately with experimental results.
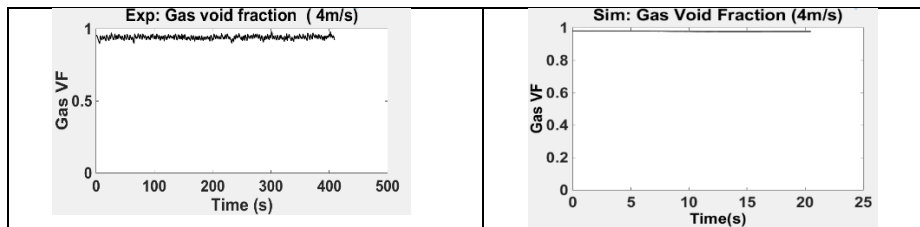
Fig. 7. Experimental and Simulation results: Liquid and gas superficial velocity: 0.05m/s & 4m/s.

5.3 Probability Density Function (PDF) Analysis

5.3.1 Superficial gas velocity of 0.1m/s.

Another approach used in this analysis is the probability density function (PDF) method. The PDF of flow regimes can be characterized by specific signatures and

peaks. Although there is a little mismatch, however, this may be due to the sampling rates. Bubbly flow is characterized by a single narrow peak (Fig. 8).
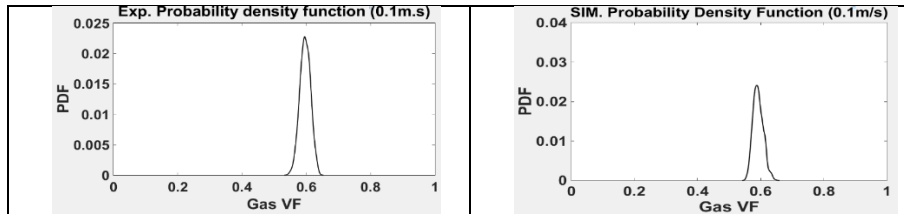
Fig. 8. Probability density function (Liquid and gas superficial velocity: 0.05m/s & 0.1m/s.)

5.3.2   Superficial gas velocity of 0.21m/s.

It was noted that there is no Slug flow in the flow regime transition due to Taylor instability as the bubble sizes covering the full diameter of the pipe cannot be developed. This is a notable difference between small and large diameter pipes. According to [20], a typical PDF curve of churn flow is a single peak slanted downwards, with average VF of 0.7 and 0.85, similar to the observation in the simulation and experimental results (Fig. 9). A slug flow would have exhibit a double peak.
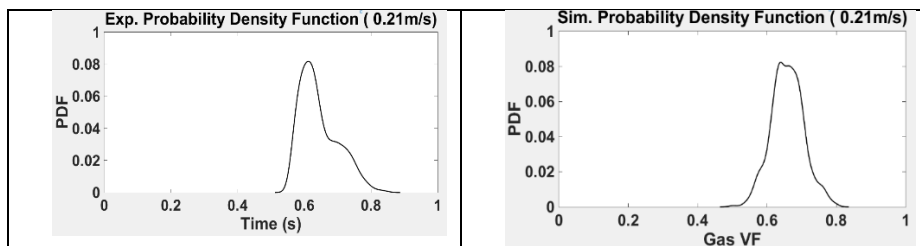
Fig. 9. Probability density function (Liquid and gas superficial velocity: 0.05m/s & 0.21m/s.)

5.3.3   Superficial gas velocity of 1m/s.

Semi annular flow is the transition range between the intermittent (churn turbulent) and the annular flow. A VF between 0.8 – 0.9 correspond to this class of regimes (Fig. 10). The discrepancy in the peak is because of the signal sampling and probably the processing kernel used.

12
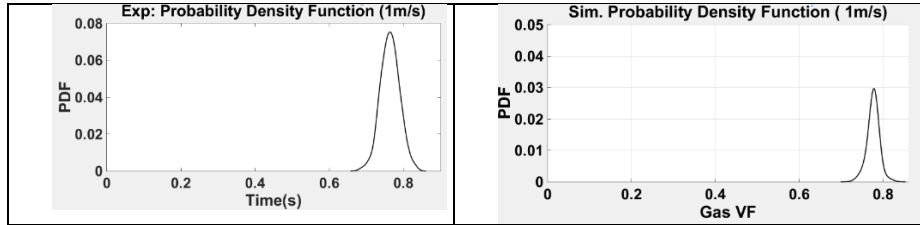
Fig. 10. Probability density function (Liquid and gas superficial velocity: 0.05m/s &1m/s.)

5.3.4 Superficial gas velocity of 4m/s.

The PDF of this simulation shows the highest peak of the signal level and often narrow peak. This correspond to between 0.85 -0.99 [20] (Fig. 11).
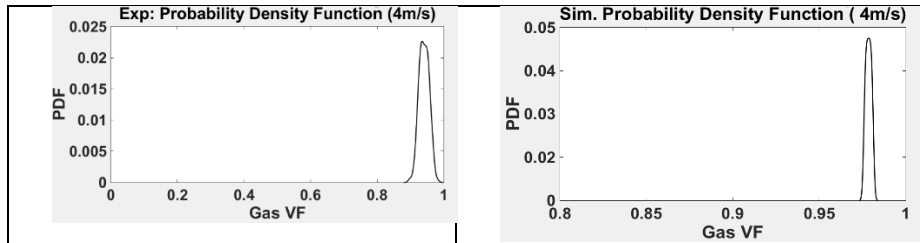
Fig. 11. Probability density function (Liquid and gas superficial velocity: 0.05m/s & 4m/s.)

A validated CFD model has been produced that can stimulate all flow regimes without prior knowledge of the flow patterns. This model is extended to investigate the impact of solid particles on the pressure gradient, liquid & gas holdup and regime transitions.

5.4   Three Phase Gas-Liquid-Solid flow simulation with CFD.

The hydrodynamics of gas-liquid-solid was investigated in this section using the CFD simulation scheme earlier validated for gas-liquid flows. The scheme was extended to investigate the impact of sand particles in the flow field and on the flow regime transitions. In this paper, only the intermittent flow is presented while further investigation is ongoing. The results showed that the presence of sand particles could change the flow dynamics and the flow regime classification and transition. The mass flux approach was used to determine the minimum mass flux threshold and deposition phenomenon. Different sand volume fractions were investigated to study the fluidization of the sand particles. The operating conditions for the churn turbulent flow investigated are listed in Table 3.

Table 3. Operation parameters for Churn Turbulent flow

Churn Turbulent (Intermittent) flow parameters					
Sand Volume fraction	5%	2.5%	1%	0.5%	0.1%
Mass flux (kg/s)	0.73	0.365	0.146	0.073	0.0146
Particle density (kg/m^3)	2500	2500	2500	2500	2500
Particles diameter (µm)	0.00025	0.00025	0.00025	0.00025	0.00025
Particle velocity (m/s)	1.3395	1.3395	1.3395	1.3395	1.3395
Gas phase velocity (m/s)	1.3395	1.3395	1.3395	1.3395	1.3395
Liquid phase velocity (m/s)	0.0593	0.0593	0.0593	0.0593	0.0593

5.4.1 Intermittent (Churn Turbulent) Case.

Five sensitives were investigated. The solid volume fraction was varied from 5% to 0.1% to determine the mass flux when sand deposition or full fluidization will occur. The results so far are shown in the contour plot of Fig. 12.

5.4.2 Sand Deposition analysis- sand void fraction

The deposition of sand particles was investigated in this section at different axial length of the flow domain. As sand particles were injected into the fluid phases, the mass flux was used as the main variable to investigate the particulate deposition and transport. Sand void fraction approach was used to determine the amount of sand left at the bottom of the pipe. The imbalance signifies the particulate deposition. Table 4 shows typical imbalance approach to determine sand deposition.

14

Sand free simulation	5% (0.73kg/s)	2.5% (0.365kg/s)	1% (0.146 kg/s)	0.5% (0.073kg/s)	0.1% (0.0146kg/s
A- No sand present- Contour plot shows churn turbu- lent regime	B- sand pre- sent- Contour plot shows churn turbulent re- gime with sand depos- ited at bot- tom	C- sand pre- sent- Contour plot changes from churn turbulent re- gime	D- sand pre- sent- Contour plot changes from churn turbulent re- gime	E- sand pre- sent- Contour plot resembles churn turbu- lent regime	F- sand pre- sent- Contour plot changes from churn turbulent re- gime

Fig. 12. Gas VF contour plots for various sand flux
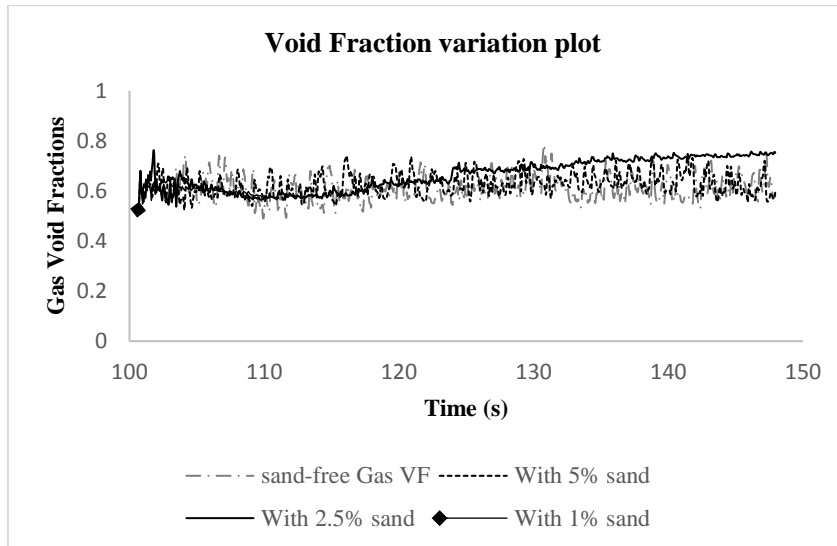
Fig. 13. Void fraction variation.

Table 4. Sand transport imbalance in pipe.

Axial position	Inlet	Outlet	Imbalance
Sand VF @ 5%	0.73	0	0.73
Sand VF @ 2.5%	0.365	7.856e-12	0.365

As shown in Fig. 12b, although the particles were fluidized but they were not fully transported to the surface. Solid phases obtained the same momentum from the gas phase but the mass flux was a determinant on the transportation of the solids (Fig. 12 c-f). The time averaged solid holdup determines the solid fluctuations and movement.

5.4.3 Mass Flux effect.

As shown in the results, the mass flux influences the hydrodynamics of the flow field. Knowing this threshold is the key to determine if deposition will occur or not at a given flow condition as listed in Table 3. As shown in Fig. 12, the mass flux determines the flow structure, gas & solid hold up distributions and the solid movements.

The solid volume fraction distribution at the bottom of the pipe is highest at 5% volume fraction which corresponds to 0.73kg/s, although, fluidization occurred, no sand was lifted to the surface above 2m axial length of the pipe. At lower sand volume fractions of 2.5% (0.365kg/s), it was discovered that some sand particles could be lifted to the surface but higher proportion of the sand were settled back at the bottom of the pipe. This is a typical case scenario of an oil well operations where sand deposition occurs at high sand flux irrespective of the flow conditions. Fig. 14 (a-d) shows the sand hold up of 2.5% volume fraction while Fig. 15 (a-c) shows the sand holdup of 1% volume fraction at different axial height.

a

b
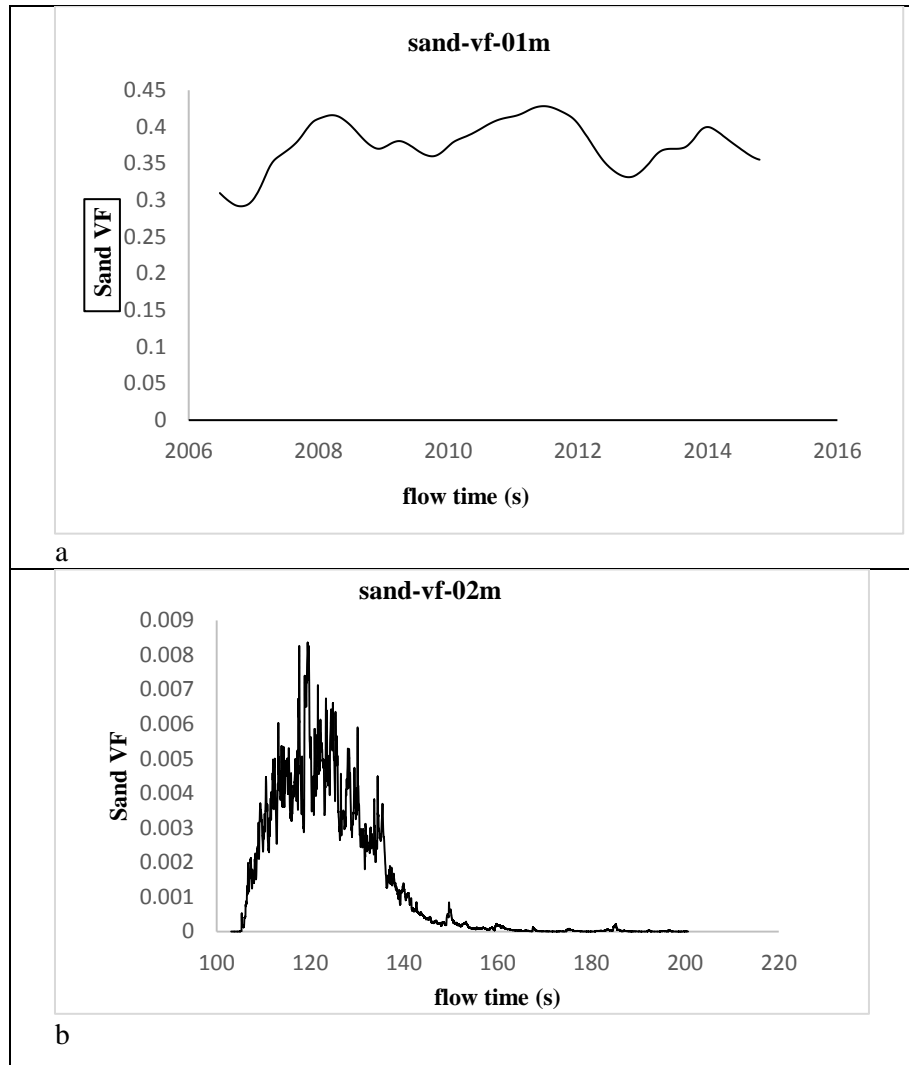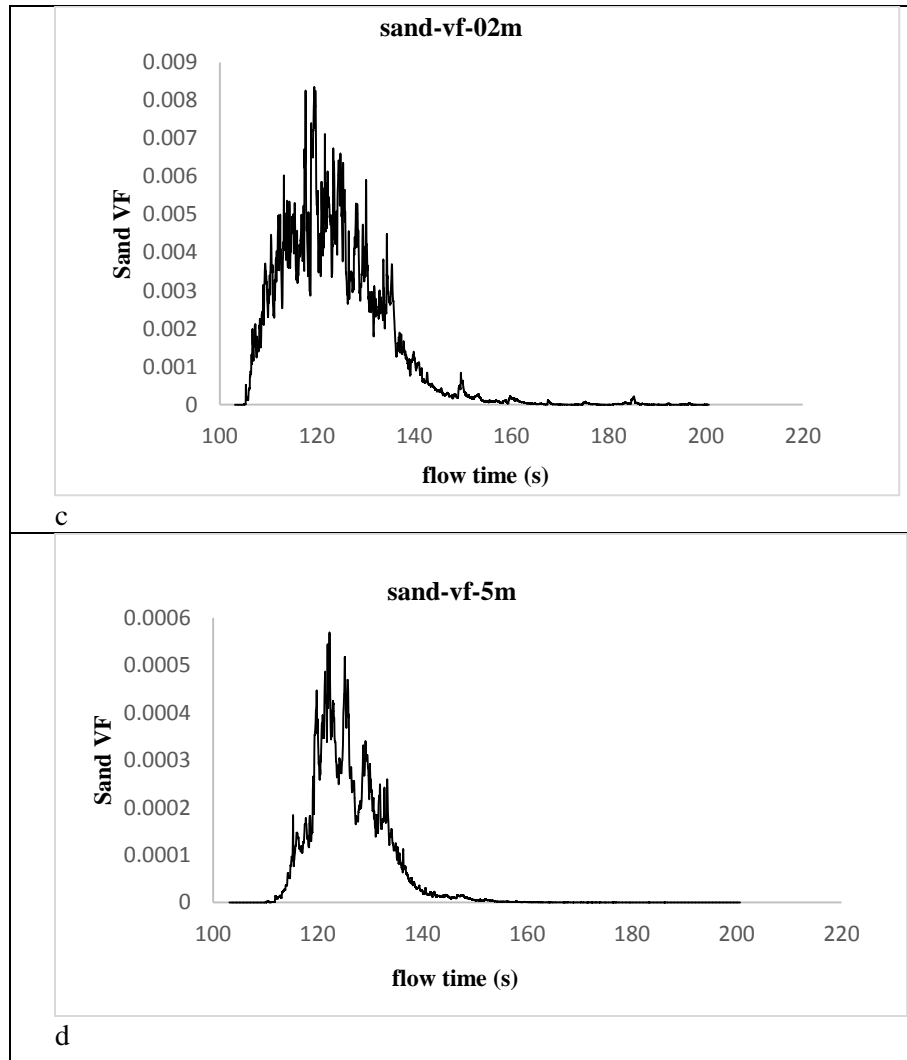
Fig. 14. Sand volume fraction: 2.5%, same velocity as carrier gas phase (1.3395m/s)

sand-vf-2m

a

sand-vf-4m

b
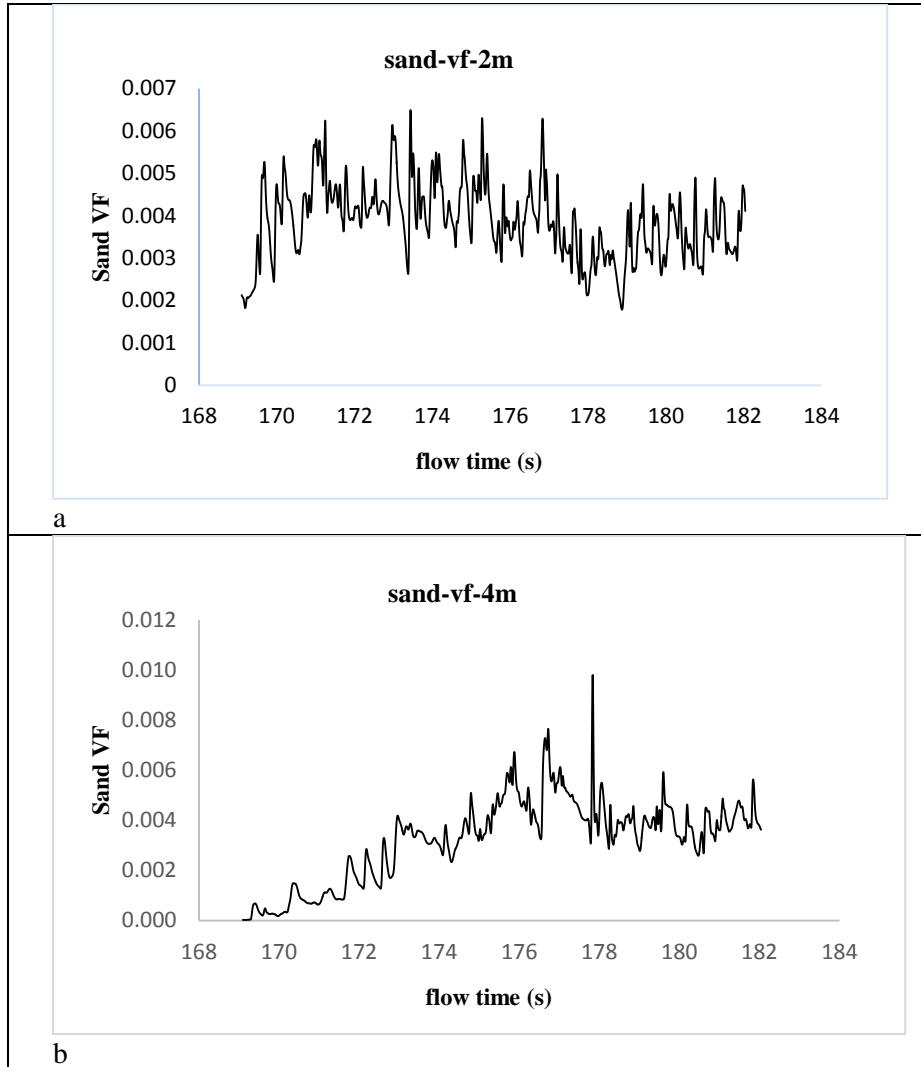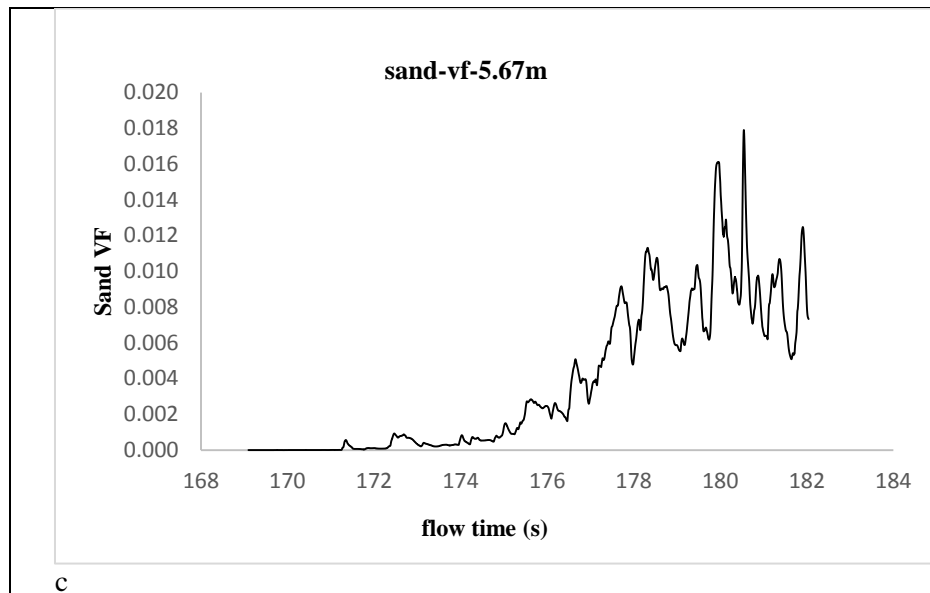
Fig. 15. Sand volume fraction: 1%, same velocity as carrier gas phase (1.3395m/s)

6   Conclusion.

CFD simulation of gas-liquid vertical pipe hydrodynamics were performed using the Euler-Euler multi-fluid volume of fluid coupled with interfacial area concentration method. The model could predict all flow regimes without prior knowledge of the flow patterns. The model was validated with experimental data and compared appropriately using the void fraction and probability density methods. The numerical scheme was extended to investigate the impact of sand particles in the flow field. The findings and key conclusions are as follows:

CFD results were compared appropriately with experimental results. The interfacial area transport equations could model the bubble coalescence and breakage, thus being able to model the flow regimes appropriately. The VF and PDF analysis method were used to analyse the similarities of results. The CFD simulation scheme could simulate the various flow regimes without prior knowledge of the bubbles sizes and void fractions.

The flow hydrodynamics of two phase gas-liquid flows is highly impacted by the presence of solid phase. The flow structure and the void fraction (bubbles coalescence and breakage) and interface of the gas bubbles were different than that of gas-liquid flow. Thus, knowledge of flow hydrodynamics of gas-liquid is not appropriate to understand gas-liquid-solid flow and cannot be used for the design of pipes where sand particles are envisage in the multiphase flow even at low concentration of solids.

The phenomenon of mass flux could be used to investigate the deposition of sand particles at the bottom of vertical pipes. The threshold of mass flux at a given flow condition is a feasible strategy to determine when sand deposition would occur. It was

evident in the foregoing that mass flux impacts the hydrodynamics transportation of gas-liquid-solid multiphase flow.

References

1. Taitel, Y., Bornea, D. and Dukler, A.E., 1980. Modelling flow pattern transitions for steady upward gas-liquid flow in vertical tubes. AIChE Journal, 26(3), pp.345-354.
2. Barnea, D., Shoham, O., Taitel, Y. and Dukler, A.E., Gas-liquid flow in inclined tubes: flow pattern transitions for upward flow. Chemical Engineering Science, 40(1), pp.131-136. (1985).
3. Brill, J.P., Modeling multiphase flow in pipes. The Way Ahead, 6(02), pp.16-17 (2010).
4. Farman Ali, S. and Yeung, H., Experimental Study of Two-Phase Air–Water Flow in Large-Diameter Vertical Pipes. Chemical Engineering Communications, 202(6), pp.823-842 (2015).
5. Johansen, S. Mo, E. Meese, J. Oliveira, J. Reyes, J. Carneiro, et al., CFD simulations of multiphase flows containing large scale interfaces and dispersed phases with selected production technology applications. In OTC Brasil. Offshore Technology Conference (2015).
6. Ohnuki, A. and Akimoto, H, Experimental study on transition of ow pattern and phase distribution in upward air-water two-phase ow along a large vertical pipe. International journal of multiphase flow, 26(3):367-386 (2000).
7. Oddie, G., Shi, H., Durlofsky, L.J., Aziz, K., Pfeffer, B. and Holmes, J.A., Experimental study of two and three phase flows in large diameter inclined pipes. International Journal of Multiphase Flow, 29(4), pp.527-558 (2003).
8. Sun, X., Smith, T.R., Kim, S., Ishii, M. and Uhle, J., Interfacial structure of air-water two-phase flow in a relatively large pipe. Experiments in fluids, 34(2), pp.206-219 (2003).
9. Omebere-Iyari, N.K., Azzopardi, B.J. and Ladam, Y., Two-phase flow patterns in large diameter vertical pipes at high pressures. AIChE journal, 53(10), pp.2493-2504 (2007).
10. Schlegel, J.P., Sawant, P., Paranjape, S., Ozar, B., Hibiki, T. and Ishii, M., 2009. Void fraction and flow regime in adiabatic upward two-phase flow in large diameter vertical pipes. Nuclear Engineering and Design, 239(12), pp.2864-2874 (2009).
11. Kaji, R. and Azzopardi, B.J., The effect of pipe diameter on the structure of gas/liquid flow in vertical pipes. International Journal of Multiphase Flow, 36(4), pp.303-313 (2010).
12. Dai, Y., Dakshinammorthy, D. and Agrawal, M., May. CFD Modeling of Bubbly, Slug and Annular Flow Regimes in Vertical Pipelines. In Offshore Technology Conference. Offshore Technology Conference (2013).
13. Smith, T.R., Schlegel, J.P., Hibiki, T. and Ishii, M., Two-phase flow structure in large diameter pipes. International Journal of Heat and Fluid Flow, 33(1), pp.156-167 (2012).
14. Pagan, E., Williams, W.C., Kam, S. and Waltrich, P.J., December. Modeling vertical flows in churn and annular flow regimes in small-and large-diameter pipes. In 10th North American Conference on Multiphase Technology. BHR Group (2016).
15. Lakehal, D., Advanced simulation of transient multiphase flow & flow assurance in the oil & gas industry. The Canadian Journal of Chemical Engineering, 91(7), pp.1201-1214 (2013).
16. Gharaibah, E., Read, A. and Scheuerer, G., October. Overview of CFD Multiphase Flow Simulation Tools for Subsea Oil and Gas System Design, Optimization and Operation. In OTC Brasil. Offshore Technology Conference (2015).
17. Gidaspow, D., Multiphase flow and fluidization: continuum and kinetic theory descriptions. Academic press (1994).

18. Ding, J. and Gidaspow, D., A bubbling fluidization model using kinetic theory of granular flow. AIChE journal, 36(4), pp.523-538 (1990).
19. Costigan, G. and Whalley, P.B., Slug flow regime identification from dynamic void fraction measurements in vertical air-water flows. International Journal of Multiphase Flow, 23(2), pp.263-282 (1997).
20. Lowe, D.C. and Rezkallah, K.S., Flow regime identification in microgravity two-phase flows using void fraction signals. International Journal of Multiphase Flow, 25(3), pp.433-457 (1999).